MODELLING OF THE 3D GLASS MELT FLOW DRIVEN BY EM AND THERMAL CONVECTION

D. Cepīte[*], Dr. A. Jakovičs[*], Dr. B. Halbedel[**], U. Krieger[**]

[*] Laboratory for Mathematical Modelling of Environmental and Technological Processes University of Latvia, 8 Zellu str., Riga, LV-1002. [**] Glass and Ceramic Technology Group Inter-faculty Institute of Materials Science Faculty of Mechanical Engineering Technical University Ilmenau, Gustav-Kirchhof Strasse - 6, D-98684, Ilmenau, Germany

Summary The main objective of this work is to develop the mathematical model, which allows to predict temperature and flow distribution in the glass melt in particular experimental set-up. The flow is iniciated due to the Lorentz force as well as by thermal convection. Ansys Cfx and Ansys Multiphysics software has been used in numerical study, which includes the coupling of electromagnetic (EM), hydrodynamic and temperature fields. Influence of external magnetic field on temperature distribution has been examined. Moreover, Ansys Multiphysics is used to ascertain that non-inductive approximation is appropriate. Numerical results are in qualitative agreement with the experiment.

1. INTRODUCTION

Stirring of a conducting melt using the Lorentz force is a well-known experimental technique. Our simulations are based on experiments done in Ilmenau Technical University showing that an external magnetic field plays an important role both in homogenisation of the temperature field and in chemical homogeneity of glass melts [1], [2]. Further unpublished series of experiments are affirming that. The proof has been obtained twofold – by direct temperature measurements on the melts axis and by the density measurements in various sections of the cooled glass. Results have been obtained in cylindrical model crucible $8\,cm$ in diameter with two rod or plate electrodes immersed symmetrically in the melt. External magnetic field with the effective induction $B=0.044\,T$ and frequency $f=50\,Hz$ is applied, to intensify and direct the flow of weakly conducting melt. Experimental technique is discussed in detail in [1]. The crucible with the melt and electrodes is inserted in insulated furnace, which is arranged in the air gap of electromagnet system. Experiments are done for the fixed Joule heat inputs $P=575\,W$ and $P=700\,W$ in the melt. One of the aims is to find out the facilities which allow getting desiderated homogeneity of temperature field by EM action. That is the reason we have decided to carry out the numerical investigation of the process.

2. MODEL

The motion of the melt is governed by the balance of the Lorentz force, thermal convection and viscous friction forces. Due to the temperature-dependent properties of the melt coupled analysis of EM, hydrodynamics and heat transfer equations should be done. The dependence was found experimentally. Temperature dependencies of electrical conductivity σ,

thermal conductivity λ, dynamic viscosity η, density ρ, specific heat capacity c_p used in our calculations are mathematically presented as

$$\rho(T) = A_\rho \cdot T + B_\rho$$
$$\sigma(T) = A_\sigma \cdot \exp\left[-B_\sigma / T\right]$$
$$\lambda(T) = A_\lambda \cdot T^{\,2} + B_\lambda \cdot T + C_\lambda$$
$$\eta(T) = A_\eta \cdot \exp\left[-1/\left(B_\eta \cdot T^{\,2} + C_\eta \cdot T + D_\eta\right)\right]$$
$$c_p = const\,,$$

where A_i, B_i, C_i, D_i are approximation constants.

We have implemented Ansys Cfx software in calculations of the problem. Mesh used in calculations consists of $\approx 2 \cdot 10^5$ elements. All imbalances below 1% and maximal residual below 10^{-5} are used as criteria for the model convergence. Hydrodynamics and heat transfer problems are implemented in the program automatically, but EM is added by adapting the transport equation to be able to solve continuity equation for the electrical current:

$$\mathrm{div}\left(\sigma(T)\,\mathrm{grad}\varphi\right) = 0\,. \tag{1}$$

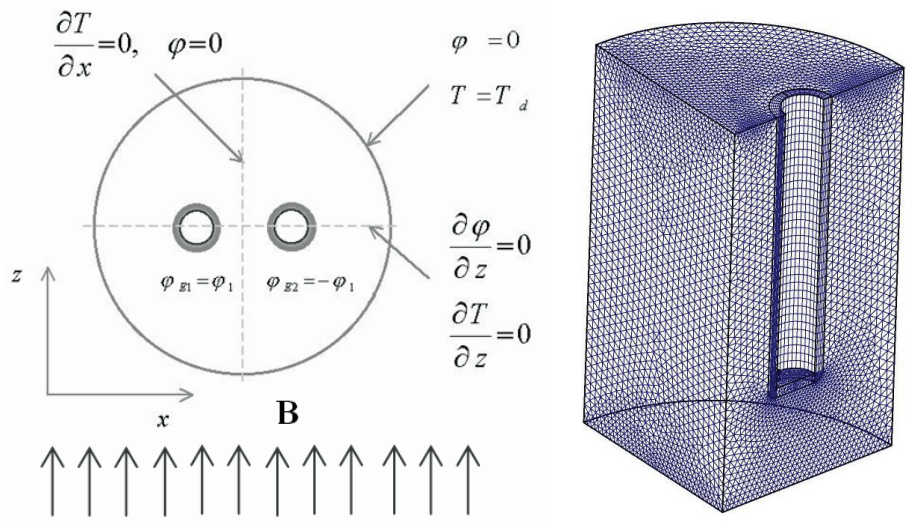

a) b)

Fig. 1. Sketch of the model with boundary conditions top view (a), one fourth part of the geometry with the mesh (b)

Top view of the geometry of the system and the boundary conditions are shown in fig.1a. Fig.1b represents one fourth part of the corresponding geometry with the mesh. High conductivity ratio $\left(\sim 10^5\right)$ between platinum (material of crucible) and the melt is kept in the sense of boundary condition - fixed value of electrical potential has been chosen on the contact surface of the melt and crucible. Due to the same reason the electrodes are assumed to be equipotent, with the effective potential $\varphi_1 = \pm U_{eff}/2$ set on the contact surface with a melt. Approach of boundary condition selection is close to that defined in our previous 2D study of the process in different geometry (the melt with plate electrodes) of the experimental set-up [3].

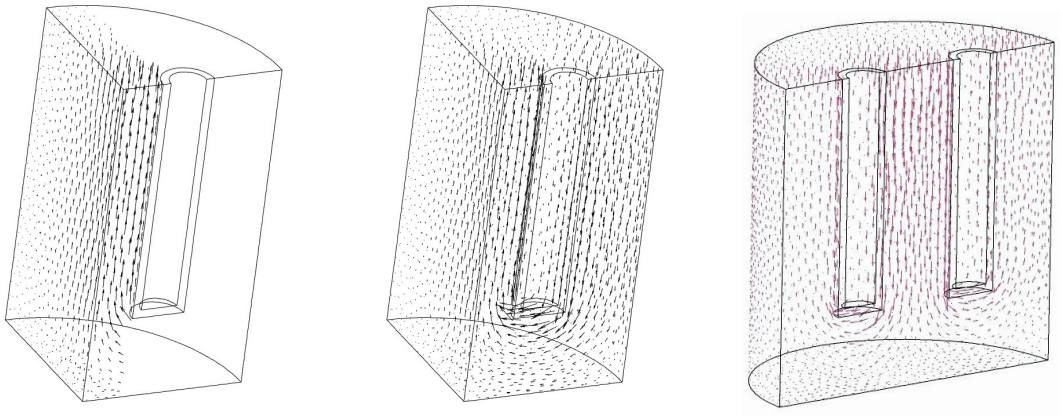

a) b) c)

0

Fig. 2. The distribution of Lorentz force in the system: a) phase angle 0 , uniform magnetic field only between the electrodes, b) phase angle 0^0, magnetic field imposed on whole melt volume, c) phase angle 180^0, magnetic field imposed on whole melt volume. Typical magnitudes of effective time-averaged Lorentz force densities are $350-500\,N/m^3$

Coupling has been established as follows – the Joule heat produced by the electrical current flowing in the melt is a source for heat transfer equation, Lorentz force density is calculated by relation $\mathbf{f}=\mathrm{Re}\left(\mathbf{j}\times\mathbf{B}^*\right)/2$ and buoyancy forces are taken into account in solving the Navier-Stokes equation. Navier-Stokes equation has been calculated in Boussinesq approximation. Heat transfer consists of heat conduction and EM and thermal convection, radiation inside the interior of the melt is negligible due to the black colour of the melt acquired by presence of Fe_2O_3 in composition of the melt. Fixed temperature is assumed on the wall of the crucible, radiation heat flux $q=\varepsilon\sigma_B\left(T^4-T_{ref}{}^4\right)$ is leaving from the top free surface of the melt, where σ_B is Stefan-Boltzman constant. After a number of numerical experiments temperature $T_{ref}=1500\,K$ has been chosen as the most appropriate for the experimental case and $\varepsilon=0.6$ has been used. Uniform magnetic field with induction in z direction is imposed on all volume of the melt. For comparison two other series of calculations have been analysed – magnetic field with induction in z direction (fig.1a) only in the region between the electrodes or there is no external magnetic field in the system. Phase shift 0 or 180 degrees is used to reverse the direction of the Lorentz force. Typical distribution of magnetic field in the melt is shown in fig.2. In case of phase angle 180^0, transient simulations have been done in one half of the system, the distribution of Lorentz force is shown in fig.2c, respectively.

It is important to justify the impact of natural Lorentz forces on the flow. It might exist due to the interaction of currents flowing in the melt and magnetic field of the currents flowing in the electrodes, and due to the changes in the distribution of the magnetic field caused by the presence of highly conducting crucible. In order to exclude the questions whether these secondary effects impact the flow additional model in Ansys Multiphysics has been developed. The distribution of EM quantities is calculated in three basic systems in case transverse magnetic field is imposed on: 1) melt with electrical conductivity σ_m (fig.3a), 2) the crucible

with electrical conductivity σ_{Pt} filled with melt (fig.3c), 3) the melt with immersed electrode with electrical conductivity σ_{Pt} (fig.3b). Magnetic vector potential formulation is used for solving the distribution of magnetic field. Full harmonic quasi-stationary analysis has been performed.

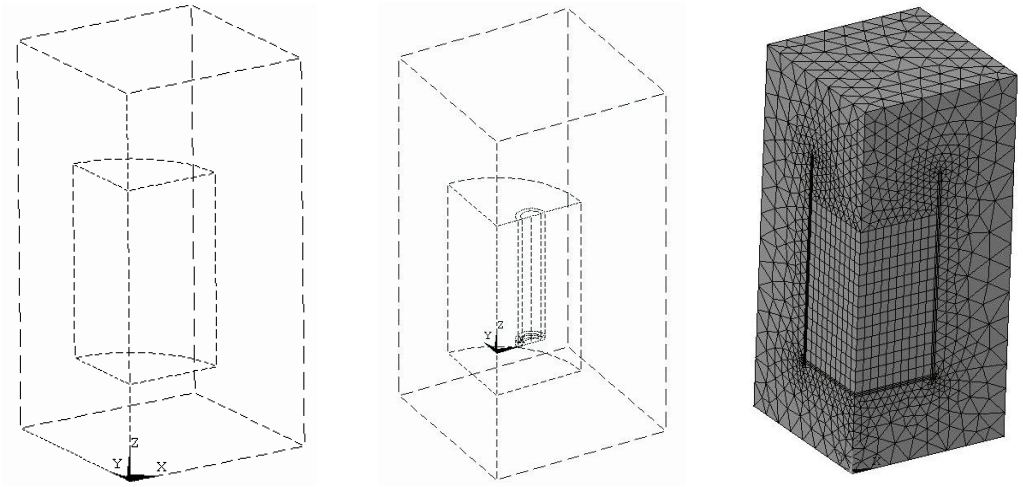

a) b) c)

Fig. 3. Geometry of models in Ansys Multiphysics: a) melt, b) melt with immersed electrode, c) melt in the crucible

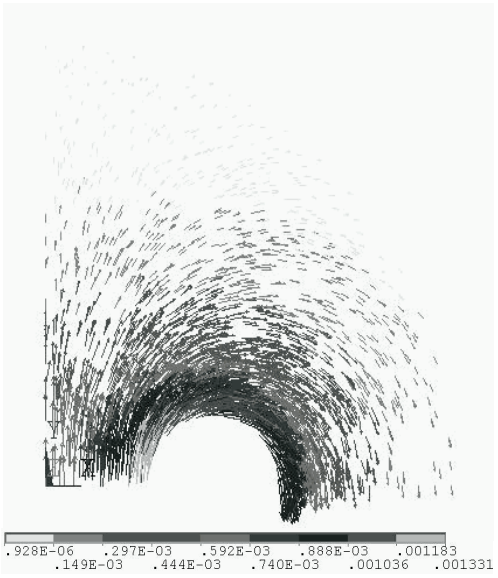

Fig. 4. Magnetic field of the electrode current in the melt – top view, T

Solution has been obtained for different parameter values of the model – different frequency and electrical conductivity of the melt. Basically the impact consists of two processes – fig.4. illustrates the distribution of the magnetic field caused by the electrode currents. In comparison with the value of external field $0.062\,T$, the maximal magnetic field around the electrodes in the melt is approximately 20 times weaker. It can be noticed that uneven decrease of the magnetic field exists around the electrode. Slower decrease of the magnetic field in the direction of symmetry plane (direction left from the electrode) can be explained with the impact of symmetrically placed second electrode. Fig.5. shows the distribution of the current density induced in the melt by alternating magnetic field. It is larger in the crucible, but in the melt it is approximately 1000 times weaker than the current flowing between the electrodes (in case of $\sigma_m = 8\,S/m$ and $U_{eff} = 27V$). Results of calculations have demonstrated that for a frequency and electrical properties of material known from the experiment changes in the amplitude of magnetic field are below 0.1% due to the presence of the crucible and the melt. Due to the magnetic field

around the electrodes the changes in magnetic field distribution approximately below 2% can be expected. Important influence (40-70% of external field's magnitude) can be prospective in case the frequency is 1000-fold increased. This result (which is also foreseeable using non-dimensional parameter non-dimensional frequency) is important to ascertain that in the particular experimental set-up the difference between the experiment and the numerical results is not related to EM assumptions, but it is related to the difference between the thermal boundary conditions in the experiment and numerical model. At the same time, the developed model might be useful for analysing the changes of Lorentz force in the system for higher frequencies.

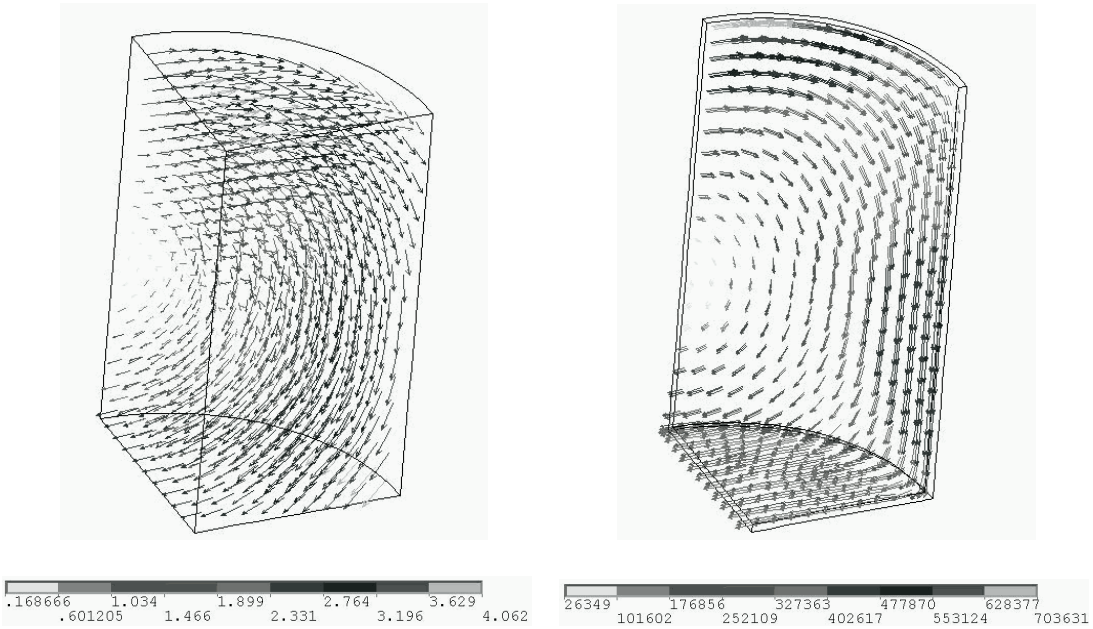

a) b)

Fig. 5. Current density distribution ($\sigma_m = 8\,S/m$, $\sigma_{Pt} = 10^6\,S/m$) : a) in the melt, b) in the crucible

3. RESULTS

The results assure that the melt flow is laminar, a typical value of the Reynolds number is ~ 1 which prevents the growth of hydrodynamic instabilities. From this point of view, calculations in a smaller region due to the symmetry are reasonable. Only the instabilities due to the coupling of temperature, velocity and Lorentz force density fields. Temperature dependence of physical properties of the melt is a reason which might intensify it. However, non-symmetric modes of instabilities are excluded from our model by calculating only the fourth part of the symmetric system. It should be pointed out that the maximum temperature in the volume according to our model is located in the central part for $B = 0$, but with $B = 0.044\,T$ the maximum temperature is located outside and it is higher than the one on the axis. It can be explained by the intensification of the upward flow in the centre, which is driven by the Lorentz force. The electric current with the highest density magnitude passes in the vicinity of the *xy*-plane between the electrodes. In this region the most intense production of the Joule heat takes

place, which results in increase of the melt temperature. The upward Lorentz force shortens the time needed for the melt to cross the central region in the *y*-direction because the melt velocity increases. The hot melt with the increasing velocity is ”brought” out of the central region and at the same time a cooler melt is ”brought” in and the Joule heat production decreases. In addition, our model shows two cases: the external magnetic field acts only in the central part of the melt and the hottest zone is located close to the melt free surface (fig.6c), but when the external magnetic field is imposed on the whole melt volume, the hottest zone moves deeper into the melt to the bottom of the electrode (fig.6b). In case of $B=0$, the velocity due to buoyancy is too low to be able to relocate the region of the maximum temperature (fig.6a).

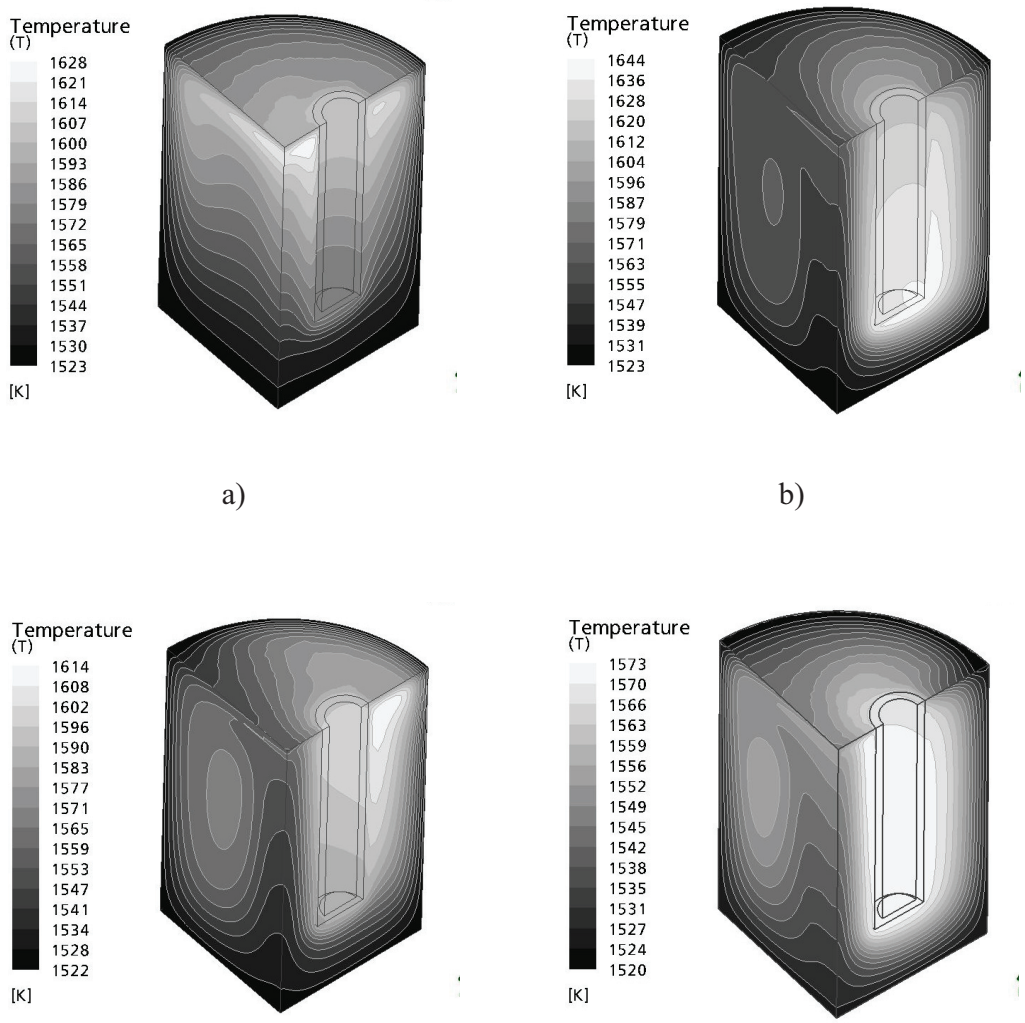

Fig. 6. Distribution of temperature in the melt: a) $B=0$, $U_{eff}=28V$ b) $B=0.044T$ in all volume of the melt, $U_{eff}=29V$ c) $B=0.044T$ in the region between the electrodes, $U_{eff}=29V$, d) $B=0.044T$ in all volume of the melt inserted in non-conducting crucible, $U_{eff}=27V$

Until now, we have no experimental data about temperatures far from the axis; this would be one of the necessary steps for the model validation and development. Additionally we have tested the impact of non-conducting crucible on the distribution of the temperature field in the melt (fig.6d). It is modeled by assuming that current does not leave the volume of the melt through its side, bottom and top. The result shows that temperature distribution around the electrodes becomes smoother, at the same time the level of temperature decreases significantly as well as the Joule heat production rate.

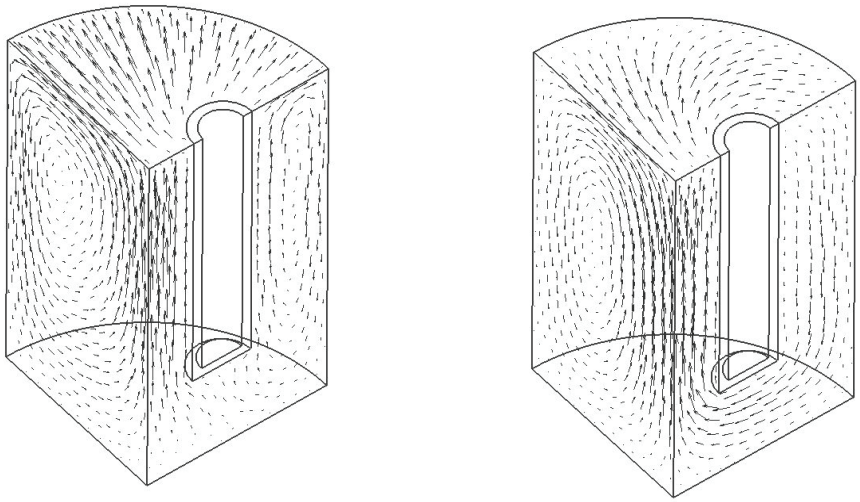

a) b)

Fig. 7. Distribution of velocity in the melt: a) $B=0$, $U_{eff}=28V$ b) $B=0.044T$ in whole volume of the melt, $U_{eff}=27V$. Maximal velocity a) $\approx 0.2 cm/s$, b) $\approx 1.2 cm/s$

The differences can be observed also in the distribution of melts velocity (fig.7). Without external magnetic field our numerical results show that the flow is directed upwards in the vicinity of the electrode. On the contrary, in case of external magnetic field applied with the phase shift $\alpha=0^0$ the flow pattern around the electrode is created with the upward motion in the central region and moving downwards in opposite side of the electrode.

In fig.8. we compare a situation, when the magnetic field is applied over the whole melt volume, with the experimental measurements. The results of our model are in qualitatively good agreement with experimentally measured axial temperature profiles. It shows that external magnetic field can be used to decrease the temperature range in the central region of the melt for a given value of the Joule heat production rate. As already seen in analysis of temperature distribution in all volume of the melt, the decrease in temperature range in all volume can be smaller than on the axis due to the fact that the hottest region is moved outside the central part of the crucible. Another point in this figure – our model shows considerably large horizontal temperature gradients, for example, both lines with scattered circles (27.5V and 27.5V (b)) correspond to the temperature measurements on two parallel axes in the central region of the melt as far as 3 mm from each other. Comparison of the results obtained on these two parallel axes allows to assume that the location of a thermoelement might impact the measurement result significantly as well as it can be seen that the experimental result lies in between experimental results.

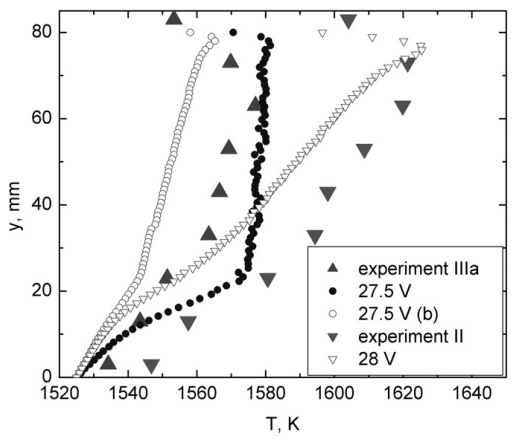

Fig. 8. Experimentally and numerically obtained axial temperature profiles, the value of model parameter U_{eff} is used in notation of numerical results. Experimental results obtained with the total Joule heat input in the system $P=575W$

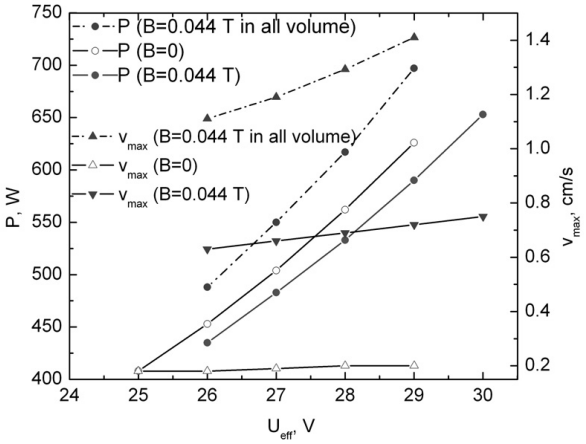

Fig. 9. Dependence of the total Joule heat input (circles) and maximal velocity (triangles) on the model parameter U_{eff} in three following cases - there is no external magnetic field, magnetic field is present only between the electrodes and magnetic field is imposed on whole volume of the melt

In fig.9. the general dependencies of our model on the parameter U_{eff} are shown in case $T_d = 1525\,K$, $T_{ref} = 1500\,K$. Dependencies are well interpretable. The highest velocities can be achieved in case the magnetic field with phase shift 0^0 is acting in all volume of the melt; it is lower in case the field is only between the electrodes and the smallest in case only thermal convection takes place. It is interesting that according to our model for a given U_{eff} the smallest Joule heat production occurs in case magnetic field is between the electrodes, it is larger in case there is no magnetic field, but in case the magnetic field is imposed on whole volume of the melt the production of Joule heat is the most intense.

It should be also stressed that our model so far is restricted to the constant temperature distribution T_d on the surface of the crucible. The constant temperature itself is a reasonable approximation due to the high thermal conductivity of platinum the crucible is made of. The point, which remains not fully understood, is the dependence of the temperature in the melt in the vicinity of the crucible bottom on the total power input. So far two experimental data sets for the particular geometry are known, which -575 W analysed here and 700 W not shown, but treated in a similar manner as shown above. The main disadvantage at the moment is that the parameter T_d should be changed empirically ($T_d = 1550\,K$) when modelling the experimental power input of 700 W), and for this reason a third experimental data set would be useful for calibrating the model until the mechanism in reality is missing.

All solutions presented above are steady-state (obtained in one fourth part of the melt volume). We have solved the problem as a transient simulation, where the stirring starts at the base temperature $T_d = 1525\,K$ for two parameter sets (with and without the external magnetic

field, respectively). Our transient simulations show that it takes up to 15 minutes for the stirring process to become stationary. The same character of the distribution of physical fields is achieved using transient and steady-state solvers. Both methods give steady-state solutions.

Different situation from those, shown in fig.6, using the external magnetic field can be achieved in case of 180^0 phase shift between the external magnetic field and current flowing between the electrodes. Equilibrium between downwards oriented Lorentz force and upwards oriented thermal convection leads to slow upwards oriented flow. Due to relatively weak velocity in the central part where the most intense currents flow it takes longer time for the melt to flow through and it is heated up more intensively. Because of intensive buoyancy the hottest region can not be moved deeper downwards. Our numerical results show that in this case the flow near the electrode on central and peripheral region is in the same direction (oriented upwards in vicinity of electrodes, fig.10b) and it is stronger in the periphery then in the central part of the crucible. On the contrary to previous results, in this case the numerical results are not able to explain the experiment. In the experiment temperature oscillations with amplitude $\approx 30K$ on the axis have been observed. That can be indicative of nonsymmetrical pulsations of the flow. More detailed analysis of conditions in real experimental set-up should be carried out to understand the differences obtained in transient numerical simulations and the experiment.

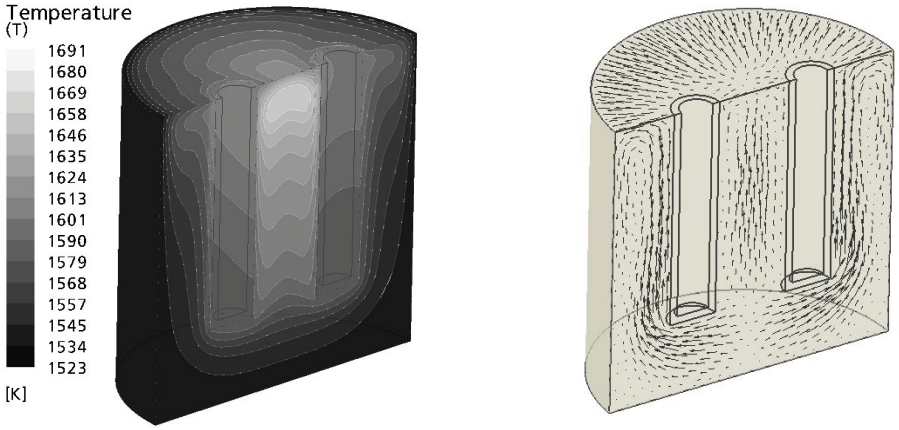

Fig.10. Temperature distribution in the system (a), velocity distribution in the system (b) in case of phase shift 180^0, Lorentz force distribution shown in fig.2c. Maximal velocity $\approx 0.2\,cm/s$

CONCLUSIONS

1. It has been shown that mathematical model describes qualitatively well the experimental results. Application of transverse external magnetic field is able to diminish the temperature range on the axis of the crucible. Moreover, insight of probable temperature distribution in all volume of the melt has been given. Numerical analysis shows large horizontal temperature gradients in the central part of the crucible which should be taken into consideration while interpreting the experimental results.

2. According to our numerical results, temperature distribution on the crucible axis is not fully representative for characterisation of temperature field in the melt.
3. Additional EM model in Ansys has demonstrated that it is beyond all doubt that secondary EM effects can be neglected in the modelling of the system. Further development and validation of the model should be related to more detailed analysis of thermal boundary conditions on the surfaces of the melt. For example, finding appropriate mechanism of interrelation between the Joule heat input and thermal boundary conditions on the crucible walls can be used to reach better quantitative agreement between numerical and experimental results.

Acknowledgements

The work is carried out in Latvia University and has been supported by European Regional Development Fund (ERDF), project contract No. VPD1/ERAF/CFLA/05/APK/2.5.1./000038/020 with Latvia Central Finance and Contracting Agency.

REFERENCES

[1] Huelsenberg, D., Halbedel, B., Conrad, G., Thess, A., Kolesnikov, Y., Luedtke, U., Electromagnetic stirring of glass melts using Lorentz forces - Experimental results, *Glass Sci. Technol*. (2004), 77, No. 4, 186 – 193.

[2] Giessler, C., Sievert, C., Krieger, U., Halbedel, B., Huelsenberg, D., Luedtke, U., Thess, A., A Model for Electromagnetic Control of Buoyancy Driven Convection in Glass Melts. *FDMP*, (2005), vol 1, No. 3, 247 - 266.

[3] Cepite, D., Jakovics, A., Repsons, K., Halbedel, B., 2D Modelling of EM Glass Convection by Temperature Dependent Material Properties, *Proc. of the 4th* International Scientific Colloquium Modelling for Material Processing, (2006), June 8-9, Riga, Latvia, pp.161-166.